ELSEVIER

Nuclear Instruments and Methods in Physics Research A 443 (2000) 136–147

NUCLEAR INSTRUMENTS & METHODS IN PHYSICS RESEARCH Section A

www.elsevier.nl/locate/nima

UV-enhancement of photomultiplier response: a study of wavelength shifters for the AMANDA/IceCube detector

P. Bauleo[1], A. Goobar*, J. Rodríguez Martino

Department of Physics, Stockholm University, Box 6730, S-11385 Stockholm, Sweden

Received 5 March 1999; received in revised form 18 August 1999; accepted 2 September 1999

Abstract

Wavelength shifters have been tested to investigate the enhancement of the sensitivity of AMANDA/IceCube optical modules to Cherenkov light. An improvement in signal detection can be achieved by adding a layer of material in front of the detector that is capable of absorbing light in the wavelength interval 200–350 nm, and re-emits it within the region of maximum response of the photomultiplier, i.e., ~ 400 nm. Two chemical compounds were found to be very suitable: an increase in light detection efficiency by more than 40% was measured, while the time resolution of the detector is only worsened by less than 3 ns.

PACS: 95.55.Ry

1. Introduction

1.1. Motivation

The Antarctic Muon And Neutrino Detector Array (AMANDA) telescope is under construction deep in the ice of the glacier at the Amundsen-Scott station, placed at the geographic South Pole [1]. The purpose of the experiment is to detect Cherenkov light produced in the ice by highly relativistic muons and other charged particles originated in cosmic–neutrino interactions. The detector consists of an array of hemispherical 8″ photomultiplier tubes (PMT), arranged in several strings and buried between 800 and 2000 m below the surface of the ice. In the future, more strings will be added to build a detector with a volume of 1 km^3 (IceCube).

The intensity and arrival time of the light are used to reconstruct the trajectory of the charged particles, and relate it to that of the original neutrino.

To prevent damage, each PMT is mounted inside a spherical pressure vessel made of glass. The photocathode is in mechanical and optical contact with the sphere through a silicon gel (General Electric RTV6156). The whole set is often referred to as optical module (OM).

The transmission of the glass (Benthos sphere) in the range 380–440 nm is $\gtrsim 80\%$ and the 50% cut-off in the UV range is at ~ 340 nm, as shown in Fig. 1. The absorption of light by the gel is

* Corresponding author. Tel.: + 46-8-164725; fax: + 46-8-347817.

E-mail addresses: bauleo@tandar.cnea.gov.ar (P. Bauleo), ariel@physto.se (A. Goobar), julio@physto.se (J. Rodríguez Martino).

[1] Permanent address: Laboratorio TANDAR, Comisión Nacional de Energía Atómica, Av. del Libertador 8250, (1429) Buenos Aires, Argentina

0168-9002/99/$ - see front matter
PII: S0168-9002(99)01007-4

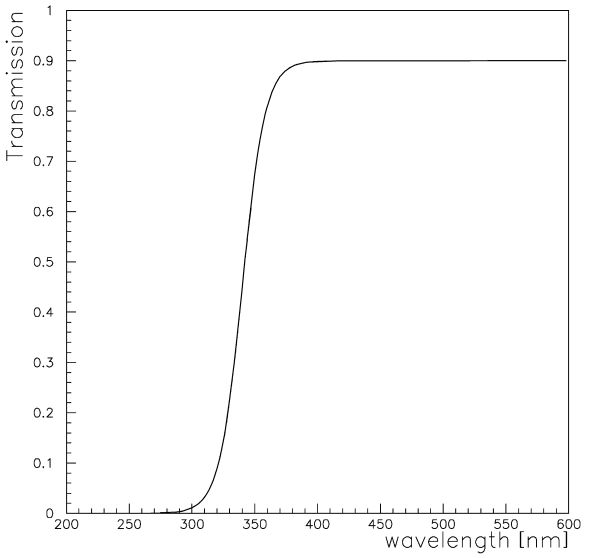

Fig. 1. Typical transmission properties of glass used in AMANDA optical modules. Photons below 300 nm are absorbed in the glass.

negligible above 300 nm. The combined effect of the absorption in the glass and in the PMT window effectively cuts out photons below 300 nm.

In this paper we investigate the use of chemical compounds, known as *wavelength shifters* (WLS), that absorb UV-photons and re-emit in the visible regime. WLS have been used extensively in water Cherenkov detectors, both dissolved in water [2] or using plastic materials doped with WLS [3]. They have also been deposited by evaporation on the PMT glass surface, with excellent results [4]. In this work, the WLS have been dissolved and painted over the OM surface (see Section 2 for details). Since Cherenkov radiation is emitted predominantly in the UV part of the electromagnetic spectrum, an increase in the collected light is expected. However, it is also important for the WLS used to have good light transmission properties in the range of wavelengths where the PMT is sensitive, to avoid absorption of visible photons.

Unlike some previous studies on the subject (e.g. Ref. [4]), this work is focused on the wavelengths ranging from 200 to 600 nm. The light absorption in polar ice makes measurements below that range of no practical interest (see Section 1.2).

Earlier laboratory studies within the AMANDA collaboration [5,6] showed an increase in light collection from Cherenkov radiation from cosmic ray muons, when painting the outer surface of the glass spheres of the OM with WLS. We have verified the results of Ref. [6] and studied the wavelength sensitivity of that painted OMs. In addition, we have measured the timing deterioration due to the finite re-emission time of the WLS.

The painting method showed inappropriate to resist the extreme conditions of the detector environment (see Section 4.3). For this reason we chose to concentrate our efforts in finding the WLS that best fits our needs. In a future study the mechanical resistance problem should be investigated.

1.2. Optical properties of South-Pole ice

Measurements of the optical properties of the South-Pole ice indicate that the glacial ice is extremely transparent [7–9]. At 415 nm, for example,

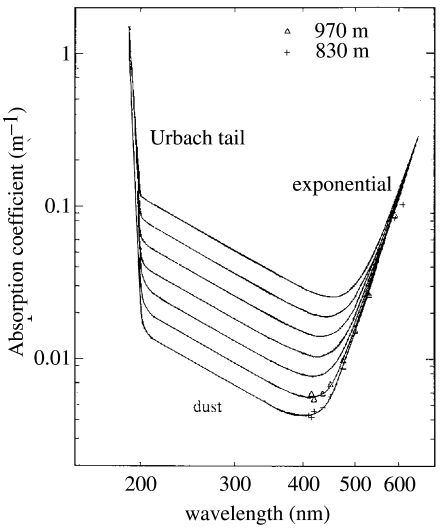

Fig. 2. Three-component model of absorption by ice containing insoluble dust but no dissolved impurities. The concentrations of dust increase by factors of 1.4 for each curve. The experimental points shown correspond to measurements made with the AMANDA detector at two different depths. Reproduced from Ref. [9][2].

[2] We have corrected a mistake in the original version where the wavelength scale was erroneously labeled as μm instead of nm.

the absorption coefficient at a depth of 800 m is only 4×10^{-3} m^{-1}, as shown in Fig. 2. At greater depths, a varying density of dust particles increases the absorption coefficient. The minimum absorption coefficient in the region of the AMANDA B13 detector (centered at 1700 meters) is approximately 0.01 m^{-1}. The curves in Fig. 2 can thus be used to extrapolate the absorption properties to the UV-region. For $\lambda \geq 200$ nm the absorption length is expected to exceed 30 m.[2] The scattering properties of the ice, measured by the AMANDA collaboration in the wavelength range 337–510 nm, are expected to depend only weakly on the photon wavelength above 200 nm [10,11]. In summary, an increase in wavelength sensitivity of the optical modules should greatly enhance the effective area of the detector.

1.3. General properties of wavelength shifters

The AMANDA detector measures Cherenkov light, which has an emission spectrum inversely proportional to the square of the photon wavelength [12]. For the current AMANDA OMs, a great fraction of photons cannot be detected because their wavelengths lie in the range where the convolution of PMTs quantum efficiency and glass transmission vanishes. An improvement in signal detection can be achieved with a suitable WLS that absorbs light between 200 and 350 nm, re-emitting it within the region of maximum response of the PMT, i.e. ~ 400 nm.

Since time measurements are crucial for reconstructing the direction of the particles crossing the detector, the timing properties of the PMT signal are of special interest. These properties are modified by the fluorescence lifetime (τ_0) of the WLS. The intensity of the re-emitted light decays exponentially with time and τ_0 is defined as the interval during which that intensity has fallen to a value $1/e$ of its maximum value.

Another important property of a WLS is the quantum yield (Q), which is the ratio of re-emitted to absorbed photons. The energy of the absorbed photons can be dissipated by other processes than the emission of visible light, for instance internal conversion, rotational and vibrational modes, etc. The quantum yield measures the amount of energy re-emitted into light. It should be noted that the quantum yield is not only an intrinsic property, but

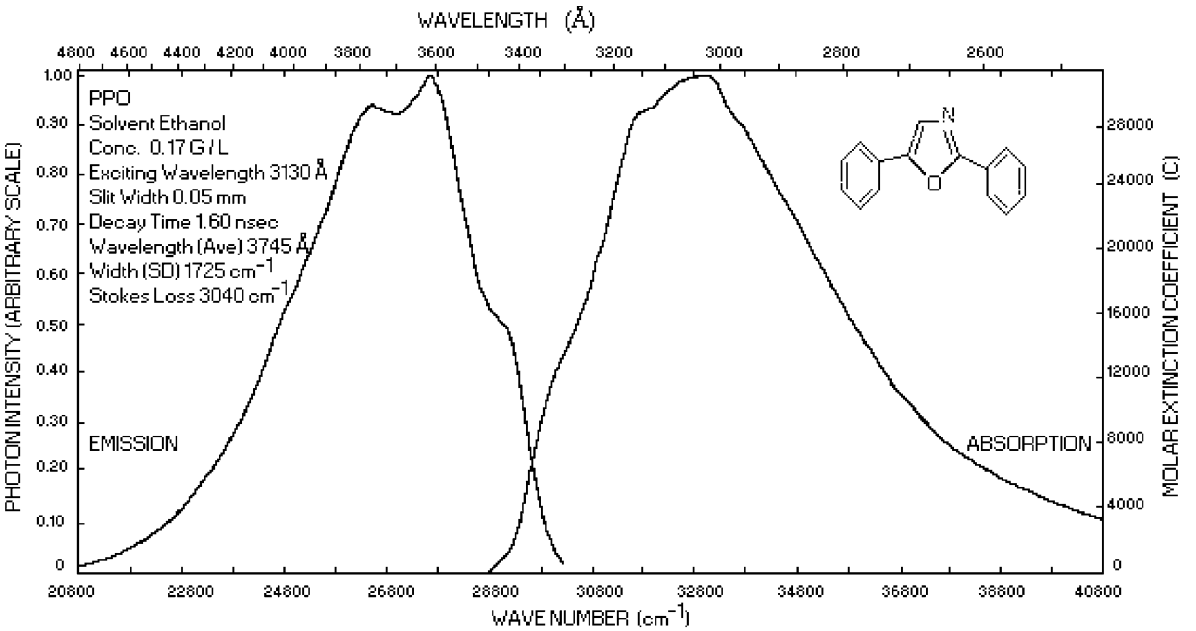

Fig. 3. Typical absorption and emission spectra of PPO. Available at http://www.pma.caltech.edu/ ~ derose/labs/exp15.html

Table 1
Properties of WLS used

WLS	k (mg/ml)	Absorbance range (nm)	Maximum reemission (nm)	τ (ns)
PPO 1	7.6	270–310	370	1.6
PPO 2	15	260–340	370	1.6
PPO 3	30	$<$ 250–345	370	1.6
PPO 4	60	$<$ 250–350	370	1.6
POPOP	18	270–385	410	1.5
PBD	9	260–330	357	1
α - NPO	10	260–360	400	2.2
PPF	33	260–350	375	1.2
Butyl-PBD	15	?[a]	?[a]	?[a]
Butly-PBD	15	?[a]	?[a]	?[a]
P-terphenyl	5	250–300	340	0.95
POPOP	2.5	330–365	410	1.5
PMP	15	?[a]	?[a]	?[a]
P-terphenyl	5	250–300	340	0.95
α - NPO	6	300–360	400	2.2
P-terphenyl	5	230–300	340	0.95
POPOP	4.5	320–380	410	1.5
PPF	3.3	300–340	375	1.2
P-terphenyl	5	250–300	340	0.95
POPOP	4	330–380	410	1.5

Concentration of Paraloid Binder: 25 mg/ml.
[a]The question marks indicate that no information was avialable for those compounds.

also depends on the concentration of WLS and the solvent medium, which may inhibit or enhance some of the mentioned processes.

The different possible routes of losing excitation energy also affect the measured decay time. The pure natural fluorescence lifetime (τ_0) is related to the measured decay time (τ) by the expression:

$$\tau_0 = \frac{\tau}{Q} \tag{1}$$

It is thus possible to obtain different decay times for the same WLS by changing the concentration.

The last property of interest is the molar extinction coefficient (ε) which is related to the probability of light absorption of the WLS:

$$\varepsilon = \frac{\log_{10}(I_0/I)M}{kd} \tag{2}$$

where I_0 is the amount of light incident on the sample, I is the amount of light transmitted by the sample, M is the molecular weight of the compound, k is the concentration in mg/ml and d is the thickness of the layer in cm ($\sim 10^{-2}$ cm).

Fig. 3 shows the absorption and re-emission spectrum of PPO, one of the tested WLS. The absorption spectrum is related to ε using the vertical scale and the WLS concentration needed to assure the desired value of absorption in a certain wavelength range can be calculated.

The typical values of the absorption range for the compounds tested in this work are 230–350 nm. The average wavelength of the re-emitted light ranges from 350 nm to 420 nm approximately. The fluorescence lifetimes are less than 3 ns and the quantum yields are greater than 0.8. An extensive description of the mentioned properties can be found in Ref [13].

2. Wavelength shifters tested

The choice of the different compounds tested was based on the absorption and re-emission properties discussed in the previous section.

The amount of WLS used in each case was calculated according to Eq. (2) and data from Ref.

[13], in order to assure 99.9% of light absorption in the interesting wavelength range with a layer thickness of approximately 10^{-2} cm.

Most of the compounds tested had their maximum reemission close to 400 nm, where the PMTs sensitivity has a maximum. In some cases, when the value of the maximum re-emission wavelength was lower, a second compound was used to absorb the light re-emitted by the first, trying to convert this light into visible photons.

For each test, the corresponding amount of WLS was dissolved in 5 ml of dichloromethane. A plastic material (Paraloid binder) was added to this solution to provide some mechanical support to the WLS. The optical properties of this binder were tested and we found very low or negligible absorption in the wavelength range of interest (see Section 3.5). The solution was hand-painted over the OM glass sphere using brush, allowing it to dry for about 15–20 h.

The properties of some of the compounds used were unknown to us. These are indicated with a question mark in Table 1. In those cases, the amount of WLS used was chosen to be similar to that used for the other compounds.

PPO was chosen to test how the properties of the same WLS change with different concentrations. The reason for this choice is that this compound was used with good results in a previous work [6].

3. Measurements

3.1. The test setup

The first task was to find out which of the different compounds gave an increase in the charge collected, using as a reference the corresponding OM without painting. For this purpose an OM was enclosed inside a dark stainless-steel tank, and illuminated through a quartz glass window using an hydrogen flash lamp. The light beam was filtered using a monochromator ($\Delta\lambda < 5$ nm). The charge spectra corresponding to different wavelengths were recorded using a LeCroy 2249W ADC.

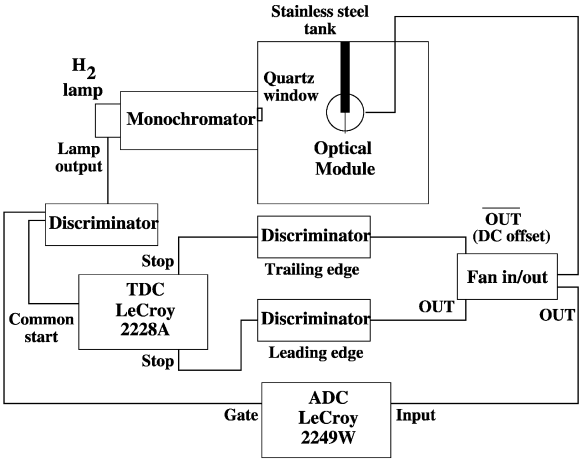

Fig. 4. Schematic view of the experimental setup used to measure the charge collected and the time distribution of pulses.

The analog output of the lamp generates a sharp signal (~ 1 ns) for each flash, and was used to generate a digital pulse applied to the common start input of a LeCroy 2228A TDC. The time intervals between the trigger pulse from the lamp and the leading and trailing edges of the PMT pulse were recorded.

Two OMs were alternatively used and a set of reference measurements was taken for each of them. For the time measurements the output slit of the monochromator was adjusted to obtain a time spectrum corresponding to single-electron pulses. Assuming Poisson statistics and the fact that about 85% of the recorded events have no signal in the PMT, we estimate that 14% are 1-photoelectron events and only 1% were due to multi-photoelectron hits. When the OM was painted with WLS the time spectrum was recorded at 240 nm to assure that the measured time distribution corresponds only to photons re-emitted by the compound. The uniform contamination from PMT noise pulses was negligible in all the measurements. A schematic view of the experimental setup used is shown in Fig. 4.

3.2. PMT linearity corrections

Since the charge collected in several measurements is to be compared in this experiment, it is of

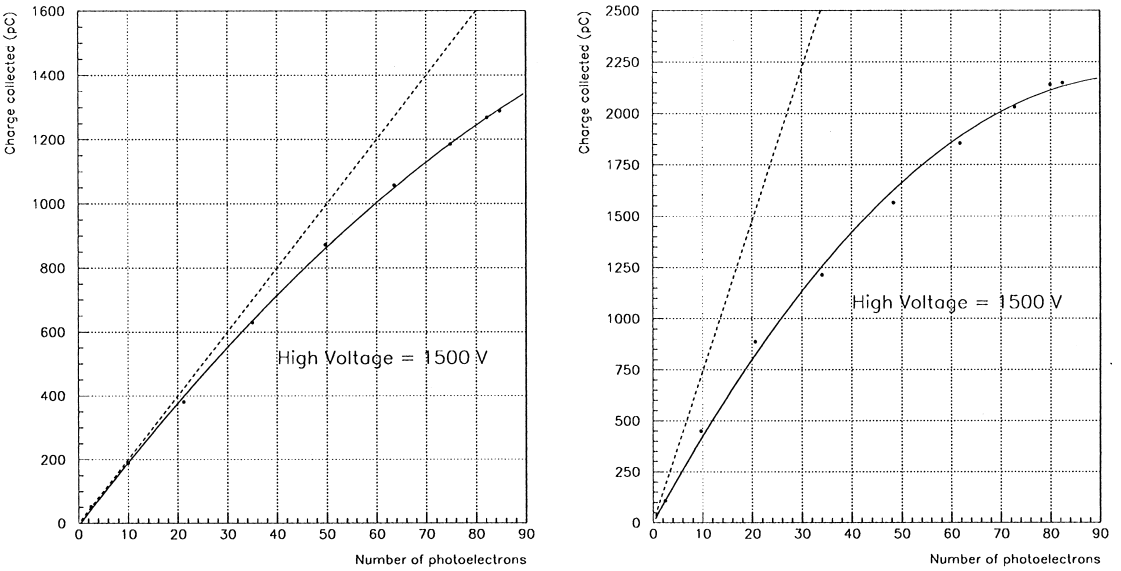

Fig. 5. Linearity test of the PMTs used. The solid lines are polynomial fits to the experimental points, used to correct the measured values of collected charge. The dashed lines represent the ideal linear behavior of the PMTs, and were calculated using single-PE measurements.

paramount importance to assure that the PMTs are working within their linear response range. Or, at least, it is necessary to know how much their response deviates from the ideal one, in order to correct the measured charge values. The linear range of the two PMTs used was tested using a very simple method. The OMs were illuminated through the quartz window using the hydrogen lamp. The light was filtered using a 405 nm filter. Two polarimeters were placed between the lamp and the window, in such a way that the relative angle between their maximum transmission axes could be varied and measured. The intensity of the transmitted light can be calculated using:

$$I = I_0 \cos^2(\theta) \tag{3}$$

where I is the measured light intensity, I_0 is the light intensity transmitted when the polarimeters axes are aligned and θ is the angle between the axes. The charge value measured as a function of the number of photoelectrons (PE) is shown in Fig. 5. The solid lines are polynomial fits to the experimental points, used to correct the measured values of collected charge due to nonlinearity of the PMTs. Previous measurements of the single-PE spectrum were used to convert the relative light intensity into PE in the horizontal scales, and to calculate the ideal linear response of the PMTs, showed as dashed lines in the plot.

It can be noted from the plots that even when the two PMTs are of the same type (Hamamatsu R5912) and are operated at the same voltage, their behavior is quite different.

3.3. Decay time

The experimental set-up described in Section 3.1 was designed to measure the time interval between the lamp pulse (indicating a single flash) and the crossing of the discriminator level by the leading and trailing edges of the PMT pulse. This gives a distribution of times, which mean value is determined basically by the cable lengths. More important are the width and shape of the distribution. The time distribution of the PMTs pulses is nearly Gaussian, with a slight excess towards the larger time values. The width is given by the different

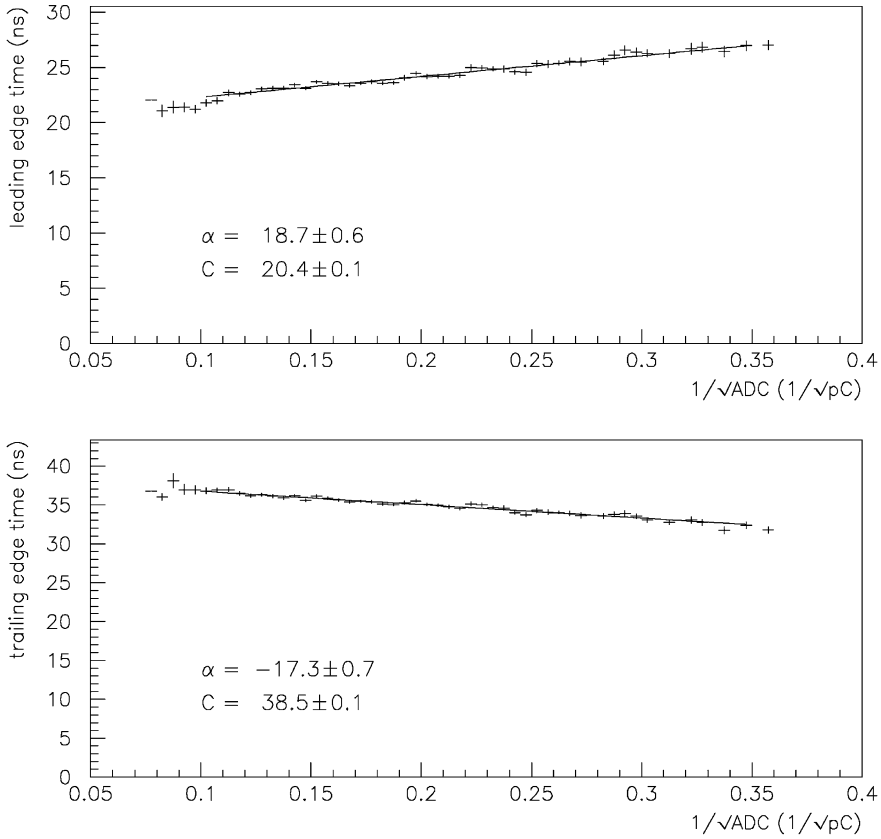

Fig. 6. Linear relation between the leading and trailing edge times and the charge values (ADC). The points plotted represent the mean value and RMS of the Y value for each value of X. The solid line is polynomial fit to the experimental data. The constants C and α were defined in Eq. (5).

paths that electrons may take to go from the photocathode to the dynode chain, inside the PMT [14]. This generates the asymmetry: there is a minimum time for the electron to reach the first dynode, but there are many other longer paths.

Some small contribution can be expected from the lamp decay time, but it was found to be negligible when compared to the WLS decay time. That means that the time distribution when the OM is painted with WLS is modelled as a convolution product between a Gaussian function and an exponential decay

$$N(t) = A\int_0^{\infty} \mathrm{e}^{-(t-t'-t_0)^2/2\sigma^2}\,\mathrm{e}^{-t'/\tau}\,\mathrm{d}t' \qquad (4)$$

where $N(t)$ is the number of counts observed at time t, A is a normalisation constant, t_0 is the distribution centroid, σ is the width of the Gaussian distribution and τ is the decay time.

The integral in Eq. (4) was solved analytically and used to fit the measured time distribution for the reference measurements.

In the cases when we used more than one WLS, the decay time is a combination of the different decay times of each compound. For simplicity, we treated those cases as if we had only one effective decay time. This is sufficient for the purposes of the AMANDA experiment, as we are only interested in the total contribution to the time spread, and not in the individual decay times.

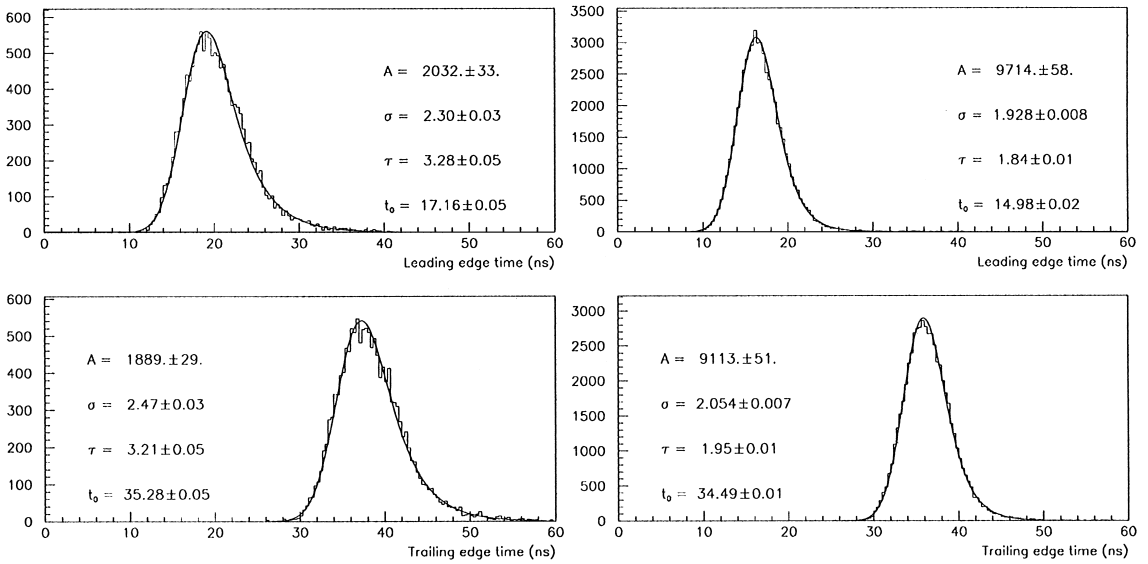

Fig. 7. Time spectra of the same OM painted with WLS (left) and clean (right). The distributions of leading and trailing edge times, corrected by time jitter as explaind in the text, are shown in the upper and lower plots, respectively. The values shown correspond to the fit of the function in Eq. (4) to the experimental data and errors are given by the fitting routine used.

Since we used a fixed discrimination level, some time jitter due to pulses with different amplitude can be expected [12]. The leading edge time (LE) measured can be written as

$$\mathrm{LE} = \frac{\alpha}{\sqrt{\mathrm{ADC}}} + C \tag{5}$$

where α and C are constants to be fitted using experimental data. ADC is the measured value of the charge given by the PMT pulse. The constant C represents the mean value of the leading edge time for an infinitely large value of ADC. An identical equation holds for the trailing edge (TE) time. Typical plots of leading and trailing edge times are shown in Fig. 6.

Once the values of α are obtained from the fits, the LE and TE values are corrected to calculate the C value for each measured pulse. The shapes of the obtained distributions of C values are fitted using the function obtained from Eq. (4). Two time spectra, corresponding to the same OM with and without WLS, are shown in Fig. 7.

3.4. UV lamp calibration

The spectrum of the light source system consisting of a hydrogen lamp, a monochromator and a quartz window was measured with an UV sensitive photomultiplier (Hamamatsu R3377) and a calibrated ADC. The measured intensities were corrected according to the PMTs quantum efficiency (QE) curve, provided by the PMT manufacturer. The mean value of the charge distribution for different wavelengths (corrected for PMT QE) is shown in Fig. 8.

3.5. Transmission properties of the binder

The same PMT was used to measure the transmission of the binder used to give mechanical support to the WLS. Measurements were performed to compare the amount of light detected when painting the PMT with binder with the normal measurements. An amount of binder equivalent to that used when mixing it with WLS was used. The ratio of the charge values measured without and with binder

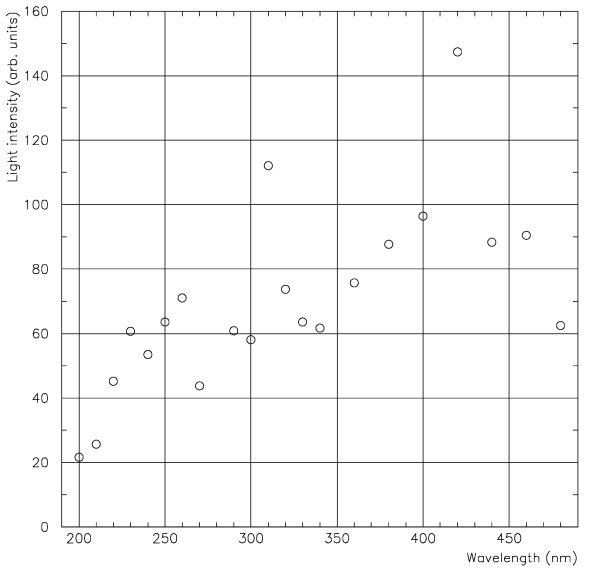

Fig. 8. Intensity spectrum of the hydrogen lamp used. The light of the lamp was filtered using a monochromator and measured through a quartz window, using a UV sensitive PMT (Hamamatsu R3377).

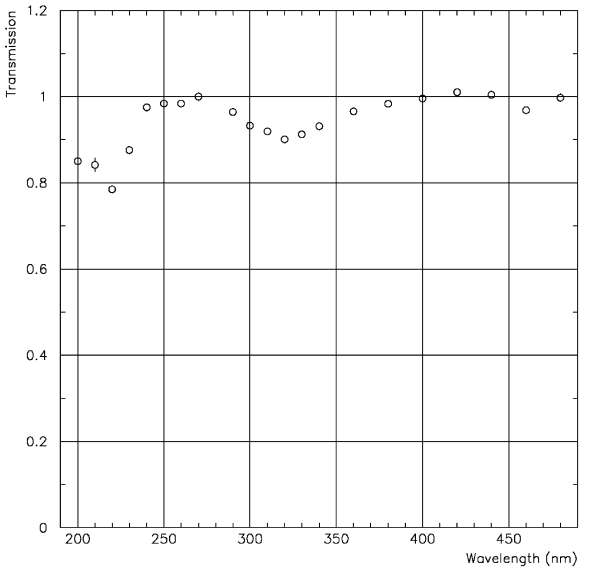

Fig. 9. Measured transmission of Paraloid binder.

was defined as the binder transmission. The obtained curve is shown in Fig. 9. The binder was found to have excellent transmission properties in the wavelength range of interest.

4. Results

4.1. Increase in light sensitivity

Charge distributions were collected with two AMANDA OMs at different wavelength for each WLS and reference runs without WLS. For each distribution (see e.g. Fig. 10), the mean value was computed and was corrected according to the relative intensity (as function of wavelength) of the light source. The resulting efficiency to light detection is a combination of the PMT QE, the absorption in the glass sphere and, for the WLS painted runs, the effect of the used compounds in converting UV light into visible photons. The relative efficiency curves for PPO and its reference are shown in Fig. 11.

While the "naked" OM is insensitive to photons below 300 nm, it can be used to detect photons with as short wavelengths as 210 nm when the glass sphere is painted with PPO. On the other hand, a fraction of photons are lost in the visible range 350–400 nm. To estimate the net gain of the WLS treatment we fold the two acceptance curves in

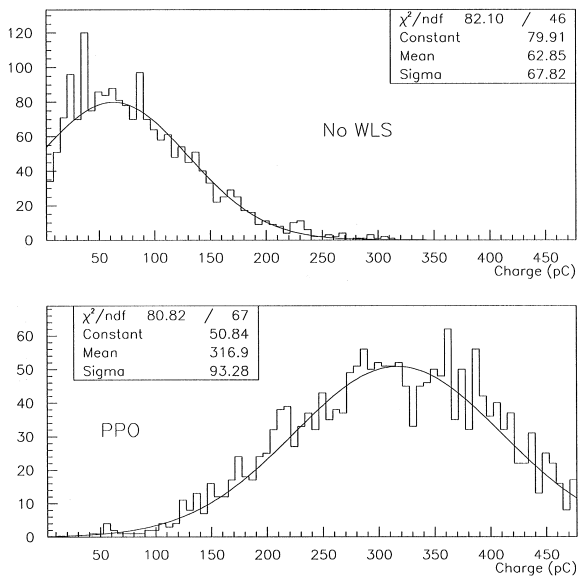

Fig. 10. Typical ADC spectra. The upper plot corresponds to the "naked" OM and the lower one to the same OM painted with PPO. Both spectra were taken at 320 nm.

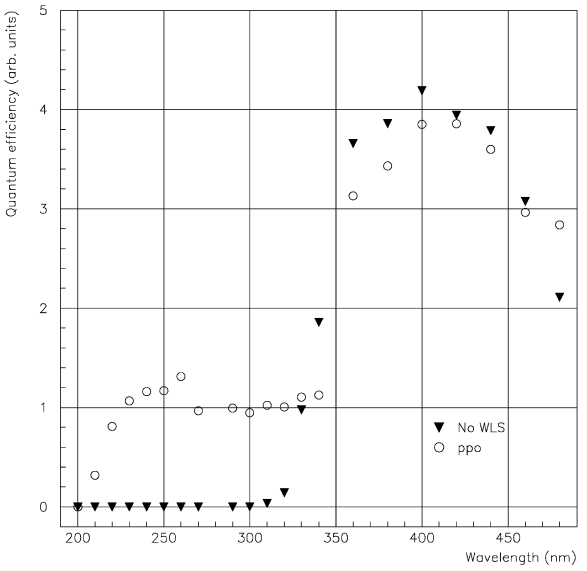

Fig. 11. Comparison of the effective quantum efficiency of a clean OM with that of the same OM painted with PPO. The concentration of this compound was 15 mg/ml.

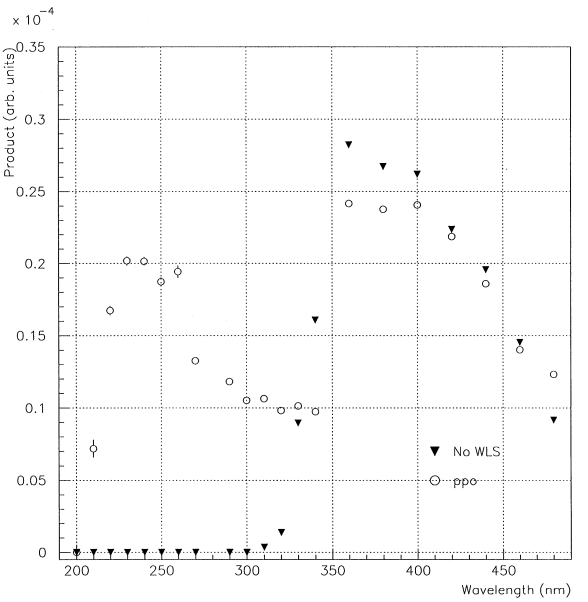

Fig. 12. Comparison of the effective quantum efficiency of a clean OM with that of the same OM painted with PPO, both corrected to take into account the shape of the Cherenkov spectrum. The concentration of PPO was 15 mg/ml.

Fig. 11 with the Cherenkov spectrum, i.e., the instrumental acceptance is weighted by the relative intensity of photons generated by the passage of a charged track, $dN/d\lambda\, dx \propto \lambda^{-2}$, as shown in Fig. 12. These curves were constructed for every WLS tested and they give a detailed description of how the wavelength sensitivity is changed.

In Figs. 11 and 12 the mean charge measured at 480 nm is larger in the case of using PPO than with the naked OM. This might be due to some UV light passing through the monocromator and contributing to the measured charge when converted to visible.

The uncertainty in the determination of the charge measured was estimated to be $\pm$ 5%. While the instrumental and analysis uncertainties are much lower than that, the main source of error has to do with the fact that the OMs were taken out of the dark tank and replaced many times, with the purpose of painting them with WLS. Due to the particular characteristics of the mounting system, they can only be placed in the same orientation with respect to the quartz window within a certain error margin. Thus, repeated exposures of the same configuration showed differences up to that value. A summary of the results of the tested compounds is shown in Table 2. The actual net gain in light collection in situ will ultimately depend on the light attenuation in the ice within the UV wavelength range.

4.2. Timing measurements

The time properties of the painted OMs were studied in special, low-intensity, exposures in order to measure a true "single photon" time distribution, as discussed in Section 3.3. The experimental distributions were fitted as shown in Fig. 7 and the decay time extracted from this fit. The fitting routine was tested using Monte Carlo generated distributions with comparable statistics as the ones in the experimental distributions. We found the results to be very robust, and accurate to about 0.5 ns. A summary of the obtained values of decay time is also shown in Table 2.

Two values are shown in the decay time column, corresponding to those obtained from the leading

Table 2
Summary of obtained values of gain and decay time "PPO after water" summarizes the results of the mechanical test described in the text

WLS	Gain (%)[a]	τ ($\pm$ 0.5 ns)	
		Leading edge	Trailing edge
PPO 1	21 ± 3	4.6	5.0
PPO 2	44 ± 5	3.3	3.2
PPO 3	45 ± 4	3.1	3.3
PPO 4	1 ± 3	3.0	2.9
PPO after water	-21 ± 3	2.9	2.8
POPOP	-1 ± 3	2.7	3.1
PBD	11 ± 4	2.9	2.9
α - NPO	8 ± 3	4.8	4.8
PPF	-1 ± 3	3.4	3.6
Butyl-PBD	41 ± 4	2.7	2.9
Butly-PBD P-terphenyl POPOP	-1 ± 3	3.2	3.2
PMP	-4 ± 3	3.8	3.7
P-terphenyl α - NPO	-12 ± 3	3.8	4.1
P-terphenyl POPOP	-28 ± 2	3.5	3.8
PPF P-terphenyl POPOP	1 ± 3	2.9	2.7

[a]All gain values are calculated by folding the acceptance curves, like those shown in Fig. 11, with the Cherenkov spectrum (see Section 4.1 for details).

and trailing edge distributions. These are two independent measurements of the same parameter.

4.3. Mechanical resistance tests

The deployment of detectors for the AMANDA telescope involves melting the glacial ice using hot water to create a cylindrical hole where the OM strings can be placed. The hole has a typical depth of about 2 km and a diameter of 0.6 m, and is filled with water coming from the melted ice. After approximately one week, the water inside the hole is completely re-frozen and the OMs are confined to their final position. The re-freezing process is critical for every component of the OM. If a painted OM is to be deployed in the future, the painting has to resist this process. The main problem in this case is that water coming from the melting of extremely pure ice, as the one present at the South Pole, is extremely corrosive.

Preliminary laboratory tests were performed to study the resistance of a WLS to this extreme conditions. The usual procedure was used to paint 15 mg/ml of PPO over an OM, which was left in contact with distilled water during approximately 72 h, to simulate to some extent the environment inside the hole. After this period, a set of charge and time measurements were performed. Results of this test are discussed in next section.

4.4. Discussion

According to our results, the WLS that best fit our needs are either PPO or Butyl-PBD. Both of them give a net gain larger than 40% and have a decay time close to 3 ns, as shown in Table 2. The optimum concentration of PPO lays between 15 and 30 mg/ml. Below this value the amount of re-emitted light is low. Increasing the concentration enhances the conversion of UV light but, at the same time, the absorption of visible light leads to a very low net gain.

All mixtures of different WLS give very low gain or even loss of charge, due to the great absorption of visible light and the poor conversion of UV light.

The obtained gain values are somewhat different to those reported in Ref. [4], where gains of up to a factor of 4 were measured when using p-terphenyl. This compound was always used in mixtures of different WLS in the present work, giving very low gain or even loss of charge, due to the great absorption of visible light. Besides this fact, the wavelength range studied is different and we also have to weight our results with the absorption in the glass sphere that protects the PMTs from pressure.

The mechanical test of PPO was not satisfactory. Parts of the painting were lost after the exposure to distilled water and the whole surface turned opaque to visible light, even to the naked eye. Further work is needed to solve this problem before being able to deploy a painted OM at the South Pole.

All the measured decay times were found to be somewhat larger than literature values. This is not surprising because our measurements are smeared

by the asymmetric time resolution of our test set-up. The combination of the time signal from the UV-lamp and the detector response shows an exponential tail also for the naked OM (see Fig. 7) which was not unfolded from the τ value. Even though, all the measured values are low enough not to affect the timing resolution of our detector.

It is worth mentioning that all measurements were performed at room temperature. The properties of WLS might change with temperature, thus some tests should be performed simulating the conditions at South Pole.

5. Conclusion

We showed that a gain of about 40% in the light collected can be achieved by using WLS, without considerably affecting the time resolution of the detector. We also made a detailed study of the OM sensitivity to different wavelengths when painted with WLS, which can be used in our simulation programs. Our results can also be applied to water Čherenkov detectors like Super Kamiokande [15] or the Auger surface detectors [16], where the water transparency can be controlled using purification methods.

More detailed studies are needed to enhance the mechanical resistance of the tested compounds. Once this problem is solved, we will be able to test the WLS in the new strings of the detector.

Acknowledgements

We are grateful to C. Spiering for providing some of the compounds used and for making available his previous work on the subject. To A. Hallgren, P. E. Tegner, M. Larsson and B. Lindgren for some of the equipment used. To L. Bergström, P. O. Hulth, A. Karle and U. Sassenberg for useful discussions. To T. Larson for some complementary measurements. To all Stockholm University workshop personnel, for their efficient work. The work of P. Bauleo and J. Rodriguez Martino was supported by a STINT Foundation fellowship.

References

[1] F. Halzen, for the AMANDA Collaboration, hep-ex/9809025; Talk presented at the 18th International Conference on Neutrino and Astrophysics (Neutrino 98), Takayama, Japan, June 1998.
[2] G. Badino et al., Nucl. Instr. and Meth. 185 (1981) 587.
[3] R. Becker-Zendy et al., Nucl. Instr. and Meth. A 324 (1993) 363.
[4] P. Baillon et al., Nucl. Instr. and Meth. 126 (1975) 13.
[5] A. Karle, private communication, Amanda Internal Note.
[6] L. Kuzmichev, B. Lubsandorzhiev, C. Spiering, Amanda Internal Note.
[7] The AMANDA collaboration, P. Askebjer et al., Science 267 (1995) 1147.
[8] The AMANDA collaboration, P. Askebjer et al., Geophys. Res. Lett. 24 (1997) 1355.
[9] The AMANDA collaboration, P. Askebjer et al., Appl. Opt. 36 (1997) 4168.
[10] A. Goobar, Amanda Internal Note.
[11] P.B. Price, L. Bergström, Appl. Opt. 36 (1997) 4181.
[12] See for example: G. F. Knoll, Radiation Detection and Measurement, Wiley, New York, Canada, 1979.
[13] I.B. Berlman, Handbook of Fluorescence Spectra of Aromatic Molecules, 2nd Edition, Academic Press, New York and London, 1971.
[14] Photomultiplier Tube, Hamamatsu Photonics K. K., Electron Tube Center, Japan, 1994.
[15] The Super-Kamiokande Detector, Proceedings of the Meeting of the American Physical Society, Division of Particles and Fields (DPF 94), Albuquerque, NM, 2-6 Aug 1994.
[16] See for example, Pierre Auger Project Design Report and references therein, available at http://www.auger.org/admin/DesignReport/index.html.